

000 001 002 003 004 005 COMMON FEATURE LEARNING FOR ZERO-SHOT IM- 006 AGE RECOGNITION 007 008 009

010 **Anonymous authors**
 011 Paper under double-blind review
 012
 013
 014
 015
 016
 017
 018
 019
 020
 021
 022
 023

ABSTRACT

024
 025 The key issue of zero-shot image recognition (ZIR) is how to infer the relationship
 026 between visual space and semantic space from seen classes, and then effectively
 027 transfer the relationship to unseen classes. Recently, most methods have
 028 focused on how to use images and class semantic vectors or class names to learn
 029 the relationship between visual space and semantic space. The relationship es-
 030 tablished by these two methods is class-level and coarse-grained. The differences
 031 between images of the same class are ignored, which leads to insufficiently tight
 032 relationships and affects the accurate recognition of unseen classes. To tackle such
 033 problem, we propose Common Feature learning for Zero-shot Image Recognition
 034 (CF-ZIR) method to learn fine-grained visual semantic relationships at the image-
 035 level. Based on the inter class association information provided by class semantic
 036 vectors, guide the extraction of common visual features between classes to obtain
 037 image semantic vectors. Experiments on three widely used benchmark datasets
 038 show the effectiveness of the proposed approach.
 039
 040

1 INTRODUCTION

041 In recent years, the development of general artificial intelligence has been rapid, and as a key link,
 042 zero-shot learning has received widespread attention. The key problem of zero-shot learning is how
 043 to infer potential knowledge between visual space and semantic space from seen categories, and then
 044 effectively transfer knowledge to unseen categories, finding corresponding semantic categories for
 045 the visual features of unseen class images, and achieving accurate class prediction of unseen class
 046 images.

047 Among the existing two types of ZSL methods, the generative model based method Wu et al. (2020);
 048 Chen et al. (2021a) learns the mapping from semantic space to visual space to generate visual fea-
 049 tures of unseen categories, thereby transforming the ZSL task into a traditional image classification
 050 task. This article believes that this method does not fundamentally solve the zero-shot problem and
 051 requires a large amount of computational resources, which is inconsistent with the original intention
 052 of the zero-shot problem. Another ZSL method, based on embedding methods Radford et al. (2021);
 053 Chen et al. (2022b); Shen et al. (2022); Wang et al. (2022), typically learns a common representation
 054 space between visual space and semantic space, where visual features and semantic vectors are pro-
 055 jected onto the common representation space, enabling knowledge transfer from seen categories to
 056 unseen categories. However, most of these embedding based methods rely on image visual features
 057 and class semantic vectors to establish visual semantic connections, ignoring the fine-grained inter
 058 class association information provided by attributes.

059 It is worth noting that most methods focus on how to use images and class semantic vectors or class
 060 names to learn the relationship between visual space and semantic space, and the relationships estab-
 061 lished by these two methods are class level and coarse-grained. The differences between images of
 062 the same class are ignored, which leads to insufficient closeness and affects the accurate recognition
 063 of unseen classes.

064 Considering the above issues, this paper proposes a Common Feature learning for Zero-shot Image
 065 Recognition (CF-ZIR) method, which guides the extraction of common visual features between
 066 categories through attributes, and simulates expert scoring to obtain the degree to which an image
 067 contains a certain attribute, thus forming an image semantic vector. Specifically, by constructing a
 068 visual attribute cross domain dictionary, guidance is provided for the extraction of visual common

054 features by attributes. At the same time, the semantic vectors of images obtained based on common
 055 visual features are constrained to be similar to the semantic vectors of their respective categories,
 056 ensuring the effectiveness of common visual features. Finally, a fine-grained visual semantic cross
 057 domain dictionary is constructed based on image visual features and image semantic vectors to better
 058 capture the fine-grained associations between class independent visual and semantic information,
 059 thus achieving high-precision zero-shot image classification tasks.

060 Our contributions in this paper are summarized as follows:
 061

- 062 • We propose the Common Feature learning for Zero-shot Image Recognition (CF-ZIR)
 063 method, which breaks new ground by discerning fine-grained visual-semantic relationships
 064 at the image level. This method leverages inter-class association information from class se-
 065 mantic vectors to guide the extraction of common visual features, leading to more nuanced
 066 image semantic vectors.
- 067 • CF-ZIR introduces a dual-layer embedding method, two layers of embeddings were estab-
 068 lished between visual-attribute and visual-semantic, respectively.
- 069 • A large number of experiments have been conducted to demonstrate that the CF-ZIR pro-
 070 posed in this chapter has achieved significant performance improvements on three bench-
 071 mark datasets.

073 The remainder of this paper is organized as follows. Section 2 introduces related work. Section 3
 074 introduces the methodology of CF-ZIR. Section 4 gives experimental results on three typical ZSL
 075 benchmark datasets. The conclusion is given in Section 5.

077 2 RELATED WORK

079 Zero-shot learning (ZSL) emerged from the challenge introduced by Larochelle et al. Larochelle
 080 et al. (2008), which questioned how to recognize images with limited labeled or unlabeled data.
 081 Lampert et al. Lampert et al. (2009) further propelled interest in ZSL within the image recogni-
 082 tion community by introducing the Animals with Attributes (AwA) dataset, built on the concept of
 083 utilizing unlabeled data.

085 ZSL diverges from conventional image recognition by enabling the identification of new class im-
 086 ages not encountered during model training, thus offering potential for numerous practical appli-
 087 cations. Existing ZSL techniques can be broadly categorized into generative and embedding-based
 088 approaches.

089 Generative methods typically address ZSL by generating samples of unseen classes to train clas-
 090 sifiers. Various methods leveraging Generative Adversarial Networks (GANs) Goodfellow et al.
 091 (2014) and other generative models have been proposed Xian et al. (2018); Ji et al. (2019); Han
 092 et al. (2021); Wu et al. (2020); Zhao et al. (2022); Chen et al. (2021a); Radford et al. (2021). Xian et
 093 al. Xian et al. (2018) presented a conditional GAN-based Mirza & Osindero (2014) approach where
 094 the discriminator was trained with class attribute classification loss, and the generator employed
 095 class attributes to produce visual features. Ji et al. Ji et al. (2019) suggested a dictionary-based
 096 method to generate pseudo-images for unseen classes, learning a dictionary for each seen class and
 097 generating pseudo-images for unseen classes by combining seen class dictionaries based on attribute
 098 distances. Recent generative ZSL methods, such as SDGN Wu et al. (2020) and FREE Chen et al.
 099 (2021a), focus on enhancing the discriminative power of generated visual features using constraints
 100 like feature refinement and self-supervised learning. However, generative methods tend to be more
 complex and computationally intensive than embedding-based approaches.

101 Embedding-based methods Jiang et al. (2018); Chen et al. (2022b); Shen et al. (2022); Yang et al.
 102 (2022); Wang et al. (2022) generally map visual features and semantic attributes into an embedding
 103 space and use distance metrics to find the closest class attributes to unseen class images. Jiang et al.
 104 Jiang et al. (2018) introduced CDL, an embedding-based method, which creates structured embed-
 105 dings and aligns visual and semantic spaces by training a coupled dictionary with visual prototypes
 106 and class attributes. Chen et al. Chen et al. (2022b) proposed a mutual semantic distillation network
 107 that builds visual-semantic embeddings from regional visual features and attribute features. Shen et
 al. Shen et al. (2022) introduced a spherical ZSL method that measures similarities in a spherical

embedding space. Wang et al. Wang et al. (2022) incorporated local image information through a fully pixel-to-attribute embedding approach.

However, existing embedding-based methods concentrate on leveraging images and class semantic vectors or class names to establish the correlation between the visual and semantic domains, inculding CLIP Radford et al. (2021) et.al cross-modal large model. These approaches typically construct relationships at a class-level, which are broad and do not account for fine-grained details. As a result, they overlook the variations among images within the same class. This oversight can lead to a lack of closeness in the learned relationships, thereby adversely impacting the precision of recognizing classes that were not seen during the training phase.

In this paper, we introduce the Common Feature learning for Zero-shot Image Recognition method, which delves into the fine-grained visual-semantic relationships at the image level. Utilizing inter-class association cues from class semantic vectors, CF-ZIR enhances the extraction of common visual features across classes, resulting in more discriminative image semantic vectors.

3 METHODOLOGY

Firstly, the task ZSL is described formally in Section 3.1. Then, the proposed framework is briefly introduced in Section 3.2. Finally, the details of training the hierarchical coupled dictionary and recognizing the unseen image are described in Section 3.3 and Section 3.4 respectively.

3.1 PROBLEM FORMULATION

The task ZSL can be described as: given a seen class sample-label set $\{(y_i^s, h_i^s)\}_{i=1}^{N^s}$, where y_i^s is a sample of seen class, and $h_i^s \in \mathcal{H}^s$ is its corresponding class label, the goal of ZSL is to predict the corresponding class label $h_j^u \in \mathcal{H}^u$ for an unseen sample y_j^u . It should be emphasized that the label set of seen classes \mathcal{H}^s and that of unseen classes \mathcal{H}^u are disjoint, i.e., $\mathcal{H}^s \cap \mathcal{H}^u = \emptyset$. Each class (both seen and unseen) is provided with a class attribute vector as available auxiliary information.

3.2 OVERALL FRAMEWORK

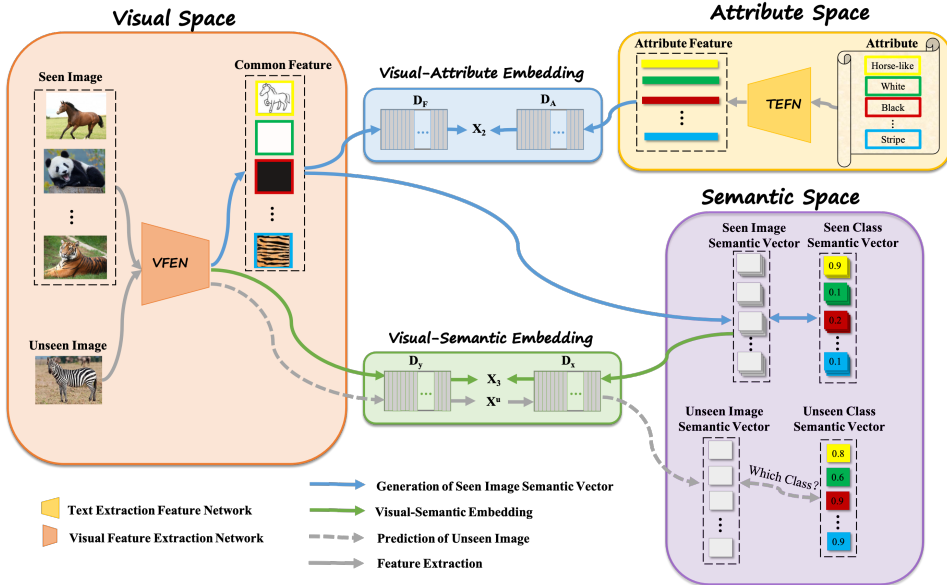


Figure 1: Framework of Common Feature Learning Zero-shot Image Recognition method. It shows the recognition performed in the semantic space based on the image-level coupled dictionary.

As shown in Fig. 1, the cross domain dictionary learning model for common feature perception proposed in this paper can be divided into two stages: visual attribute embedding stage and visual

semantic embedding stage. The gray solid line represents the feature extraction process, the blue solid line represents the model construction process in the visual attribute embedding stage, the green solid line represents the model construction process in the visual semantic embedding stage, and the gray dashed line represents the class prediction process for unseen class images.

In the visual attribute embedding stage, seen class images are first subjected to a visual feature extraction network (e.g. ResNet101) to extract visual features. The dictionary trained based on the visual features of seen class images can serve as common visual features between categories. By designing a visual attribute cross domain dictionary, the relationship between visual space and attribute space is established, which constrains the expression of common visual features and attribute features in the embedding space to be the same. In other words, common visual features are the corresponding expressions of attribute features in the visual space. Therefore, the sparsity coefficient obtained from the reconstruction of the common visual feature dictionary atom for a seen class image can describe the degree to which each attribute is included in the seen class image, that is, to obtain the semantic vector of the seen class image. By constraining the semantic vector of the seen class image to be similar to the semantic vector of the image's class, the accuracy of the common visual feature dictionary is ensured.

In the visual semantic embedding stage, the relationship between visual space and semantic space is established by constraining the seen class visual features and the seen class image semantic vectors to have the same expression in the embedding space. This relationship is class independent, so it can be generalized from the seen class to the unseen class, ensuring the model's recognition ability on the unseen class.

On the basis of the above two stages of model construction, there are three ways to predict the categories of unseen class images, namely: recognition in visual space, recognition in embedding space, and recognition in semantic space. Fig. 1 shows the process of semantic space recognition. Unseen class images obtain visual features through feature extraction networks, generate semantic vectors of unseen class images through a visual semantic cross domain dictionary, and then find the closest class to the unseen class image by calculating the distance between the image semantic vector and each unseen class semantic vector.

3.3 TRAINING OF COMMON FEATURE LEARNING ZERO-SHOT IMAGE RECOGNITION METHOD

The proposed method trains the model through two stages, including the establishment of a visual-attribute coupled dictionary and the establishment of a visual-semantic coupled dictionary.

Visual-Attribute Embedding

At the first stage, based on a single dictionary learning model, a dictionary corresponding to the visual features of a seen class image is trained, and the semantic vector of the image is generated. The formula of the loss function is as follows:

$$\mathcal{L}_{ag}(\mathbf{F}, \mathbf{X}^s) = \|\mathbf{Y}_v - \mathbf{F}\mathbf{X}^s\|_F^2 + \lambda \|\mathbf{X}^s - \mathbf{Z}\|_F^2, \quad (1)$$

where $\mathbf{Y}_v \in \mathbb{R}^{M_v \times N^s}$ is the visual feature matrix of seen images, M_v is the dimension of feature, and N^s is the number of seen images, $\mathbf{F} \in \mathbb{R}^{M_v \times K}$ is the common visual feature dictionary, \mathbf{F} contains K dictionary atoms, each atom is the description of each attribute in visual space, $\mathbf{X}^s \in \mathbb{R}^{K \times N_s}$ is the semantic feature matrix of seen images which describes the degree an image contains an attribute, $\mathbf{Z} \in \mathbb{R}^{K \times N_s}$ is the class semantic matrix of seen images.

The first constraint in Eq. 1 can reconstruct image visual features from the common visual feature dictionary \mathbf{F} and the semantic feature matrix \mathbf{X}^s , while the second constraint generates semantic feature matrix \mathbf{X}^s that are close to the corresponding class semantic matrix \mathbf{Z} , λ is a balance parameter used to adjust the contribution of the two constraints.

Extracting common visual features between categories based on attribute feature constraints, where each attribute feature corresponds to a common visual feature between categories. The formula of the loss function is as follows:

$$\mathcal{L}_{cf}(\mathbf{F}, \mathbf{D}_F, \mathbf{D}_A, \mathbf{X}_r) = \|\mathbf{F} - \mathbf{D}_F \mathbf{X}_r\|_F^2 + \mu \|\mathbf{A} - \mathbf{D}_A \mathbf{X}_r\|_F^2, \quad (2)$$

where $\mathbf{A} \in \mathbb{R}^{M_a \times K}$ is the attribute feature matrix extracted by the feature extraction network for attribute phrases, $\mathbf{D}_F \in \mathbb{R}^{M_v \times K}$ is the visual dictionary of the visual-attribute coupled dictionary,

$\mathbf{D}_A \in \mathbb{R}^{M_v \times K}$ is the attribute dictionary of the visual-attribute coupled dictionary, $\mathbf{X}_r \in \mathbb{R}^{K \times K}$ is the common description of attribute features and visual features in the embedding space, μ is a balance parameter used to adjust the contribution of the two constraints.

Totally, the loss function of the visual-attribute coupled dictionary learning stage is as follows:

$$\mathcal{L}_{att} = \mathcal{L}_{ag} + \alpha \mathcal{L}_{cf}, \quad (3)$$

where α is a balance parameter used to adjust the contribution of the two constraints.

The objective of optimization is to minimize the loss function \mathcal{L}_{att} . The variables to be solved include the common visual feature dictionary \mathbf{F} , the visual dictionary \mathbf{D}_F , the attribute dictionary \mathbf{D}_A , the semantic feature matrix \mathbf{X}^s , the common description matrix \mathbf{X}_r .

Visual-Semantic Embedding

At the second stage, align seen class images with seen class image semantic vectors by constructing a visual semantic cross domain dictionary pair. The corresponding formula is as follows:

$$\mathcal{L}_d(\mathbf{D}_y, \mathbf{D}_x, \mathbf{X}_e) = \|\mathbf{Y}_v - \mathbf{D}_y \mathbf{X}_e\|_F^2 + \eta \|\mathbf{X}^s - \mathbf{D}_x \mathbf{X}_e\|_F^2, \quad (4)$$

where $\mathbf{D}_y \in \mathbb{R}^{M_v \times L}$ is the visual dictionary of visual-semantic coupled dictionary, $\mathbf{D}_x \in \mathbb{R}^{K \times L}$ is the semantic dictionary of visual-semantic coupled dictionary, L is the number of dictionary atoms, $\mathbf{X}_e \in \mathbb{R}^{L \times N^s}$ is the description of seen image in embedding space.

The discriminant loss is adopted to further constrain the discriminability of cross domain dictionaries, the corresponding formula is as follows:

$$\mathcal{L}_q(\mathbf{Q}, \mathbf{X}_e) = \|\mathbf{H} - \mathbf{Q} \mathbf{X}_e\|_F^2, \quad (5)$$

where $\mathbf{Q} \in \mathbb{R}^{C^s \times L}$ is the discriminator, $\mathbf{H} \in \mathbb{R}^{C^s \times N^s}$ is the label matrix of seen class image.

Totally, the loss function of the visual-semantic coupled dictionary learning stage is as follows:

$$\mathcal{L}_{vs} = \mathcal{L}_d + \beta \mathcal{L}_q, \quad (6)$$

where β is a balance parameter used to adjust the contribution of the two constraints.

The objective of optimization is to minimize the loss function \mathcal{L}_{us} . The variables to be solved include the visual dictionary \mathbf{D}_y , the semantic dictionary \mathbf{D}_x , the discriminator \mathbf{Q} , the description of seen image in embedding space $\mathbf{X}_e \in \mathbb{R}^{L \times N^s}$.

Details of the training process of CF-ZIR are shown in Algorithm 1. The Line 1 to Line 7 are the visual-attribute embedding process, which includes common feature extraction and image semantic vector generation. The Line 8 to Line 13 are the visual semantic embedding process, which involves learning a visual semantic cross domain dictionary to obtain a dictionary pair. The initialization of the dictionary and classifier in algorithm is based on the KSVD algorithm, while the initialization of other variables is in the form of a random matrix.

3.4 RECOGNITION OF UNSEEN IMAGE

Based on the proposed framework, ZSL task is performed by mapping the data in visual space and semantic space into a definite space using the hierarchical coupled dictionaries. The definite space can be chosen from visual space, embedding space and semantic space, i.e., recognition in the visual space, recognition in the embedding space and recognition in the semantic space. In the following formulas, we take the recognition using image-level coupled dictionary as an example, and the class-level ones are similar.

Recognition in the Visual Space

In order to perform recognition in the visual space, the unseen class attributes \mathbf{P}_s^u is firstly mapped into the embedding space using the image-level semantic dictionary \mathbf{D}_s^{image} . The corresponding formula is as follows:

$$\arg \min_{\mathbf{X}^u} \|\mathbf{P}_s^u - \mathbf{D}_s^{image} \mathbf{X}^u\|_F^2, \quad (7)$$

where $\mathbf{X}^u \in \mathbb{R}^{L \times C^u}$ is the embedding-description of unseen classes.

270 **Algorithm 1:** Training of CF-ZIR.
 271
 272 **Input** : Seen class sample pairs (\mathbf{Y}_v, \mathbf{H}); Class attributes \mathbf{A} ; Semantic matrix of seen image
 273 \mathbf{Z} ; Hyperparameters $\lambda, \alpha, \beta, \mu$ and η ; Number of visual-semantic coupled dictionary
 274 atoms L ;
 275 **Output** : Visual-Semantic Coupled dictionaries ($\mathbf{D}_y, \mathbf{D}_x$);
 276 // Visual-Attribute Coupled Dictionary Learning
 277 1 Initialize $\mathbf{F}, \mathbf{D}_F, \mathbf{D}_A$;
 278 2 **repeat**
 279 3 Update \mathbf{X}_s via minimizing Eq. (1);
 280 4 Update \mathbf{X}_r via minimizing Eq. (2);
 281 5 Update \mathbf{D}_F and \mathbf{D}_A via minimizing Eq. (2);
 282 6 Update \mathbf{F} via Eq. (3);
 283 7 **until** maximum iteration;
 284 // Visual-Semantic Coupled Dictionary Learning
 285 8 Initialize $\mathbf{D}_y, \mathbf{D}_x, \mathbf{Q}$;
 286 9 **repeat**
 287 10 Update \mathbf{X}_r via minimizing Eq. (6);
 288 11 Update \mathbf{D}_y and \mathbf{D}_x via minimizing Eq. (4);
 289 12 Update \mathbf{Q} via minimizing Eq. (5);
 290 13 **until** maximum iteration;
 291
 292
 293

Then, the visual-description of unseen class is computed using the image-level visual dictionary \mathbf{D}_v^{image} , i.e., $\mathbf{P}_v^{u'} = \mathbf{D}_v^{image} \mathbf{X}^u$.

Finally, the cosine distance is adopted to measure the distances between the unseen image \mathbf{y}_v and the visual-description of unseen classes $\mathbf{P}_v^{u'}$, searching the class nearest to the unseen image. The corresponding formula is as follows:

$$\arg \min_{c \in \{1, \dots, C^u\}} (\mathcal{M}(\mathbf{P}_v^{u'}[c], \mathbf{y}_v)), \quad (8)$$

where $\mathbf{P}_v^{u'}[c] \in \mathbb{R}^{M_v \times 1}$ indicates the visual-description of the c th unseen class, $\mathcal{M}(\cdot, \cdot)$ indicates the cosine distance between two vectors.

Recognition in the Embedding Space

To perform recognition task in the embedding space, both the unseen image \mathbf{y}_v and the unseen class attributes \mathbf{P}_s^u are mapped into the embedding space using the image-level coupled dictionary.

The embedding-description of unseen class is computed using Eq. 7. The embedding-description of unseen image is computed using the image-level visual dictionary \mathbf{D}_v^{image} . The corresponding formula is as follows:

$$\arg \min_{\mathbf{x}^u} \|\mathbf{y}_v - \mathbf{D}_v^{image} \mathbf{x}^u\|_F^2. \quad (9)$$

Then, the cosine distances between the two embedding-descriptions are measured, and the class nearest to the unseen image is searched in the embedding space. The corresponding formula is as follows:

$$\arg \min_{c \in \{1, \dots, C^u\}} (\mathcal{M}(\mathbf{X}^u[c], \mathbf{x}^u)), \quad (10)$$

where $\mathbf{X}^u[c] \in \mathbb{R}^{L \times 1}$ indicates the embedding-description of the c th unseen class.

Recognition in the Semantic Space

To perform recognition task in the semantic space, the unseen image is firstly mapped into the embedding space using the image-level visual dictionary, shown as Eq. 9. Then, the semantic-description of the unseen image is computed by $\mathbf{y}_s = \mathbf{D}_s^{image} \mathbf{x}^u$.

The distance between each column of unseen class attributes \mathbf{P}_s and semantic-description of the unseen image \mathbf{y}_s are measured by computing the cosine distance, and the class nearest to the unseen image is searched. The corresponding formula is as follows:

$$\arg \min_{c \in \{1, \dots, C^u\}} (\mathcal{M}(\mathbf{P}_s^u[c], \mathbf{y}_s)), \quad (11)$$

where $\mathbf{P}_s^u[c] \in \mathbb{R}^{M_s \times 1}$ indicates the attribute of the c th unseen class.

324
 325 Table 1: Statistics for attribute datasets: aPY, AwA1, AwA2 in terms of the number of seen im-
 326 age (Image.S), the number of unseen image (Image.U), the dimension of class attribute (Attr.), the
 327 number of seen class (Seen) and the number of unseen class (Unseen).

Dataset	Image.S	Image.U	Attr.	Seen	Unseen
aPY Farhadi et al. (2009)	5,932	7,924	64	20	12
AwA1 Lampert et al. (2009)	19,832	5,685	85	40	10
AWA2 Xian et al. (2019)	23,527	7,913	85	40	10

333 4 EXPERIMENTAL RESULTS

336 We give experimental results in this section. We show the results on four benchmarks (Section 4.2).
 337 Then, we demonstrate the effectiveness and necessity of each part of the proposed model, including
 338 the unseen adaptation, image attribute generation, and image-level coupled dictionary (Section 4.3).
 339 Finally, we analyze the quality of generated image attributes (Section 4.4).

340 4.1 DATASETS

342 We perform experiments on four ZSL datasets including aPascal & aYahoo (aPY) Farhadi et al.
 343 (2009), Animals with Attributes 1 (AwA1) Lampert et al. (2009) and Animals with Attributes 2
 344 (AwA2) Xian et al. (2019) to verify the effectiveness of the proposed method. The statistics of all
 345 datasets are shown in Table 1. To make fair comparisons, we use the class attribute, image feature,
 346 data splits provided by Xian et al. (2017). The image features are extracted by the 101-layered
 347 ResNet He et al. (2016). Value of hyperparameters $\lambda, \alpha, \beta, \gamma, \mu, \eta$ are selected in the set {0.001,
 348 0.01, 0.1, 1, 10}. The average per-class top-1 accuracy is used to measure the performance of
 349 models.

350 The three widely used benchmarks are briefly introduced as follows:

- 352 • aPY contains 32 categories, including bird, cow, chair, bus, etc.. They belong to three
 353 major classes, i.e., animal, object and vehicle. Images and attributes in this dataset are
 354 collected from Yahoo and Pascal VOC.
- 355 • AwA1 is an animal dataset, which contains 40 seen classes, including antelope, beaver,
 356 tiger, elephant, etc., and 10 unseen classes, including sheep, seal, rat, bobcat, etc..
- 357 • AwA2 contains the same fifty animal categories as AwA1 dataset. Different from AWA1
 358 dataset, AwA2 dataset provides images collected from public sources, all licensed for free
 359 use and redistribution.

361 4.2 COMPARISON WITH STATE-OF-THE-ART

363 As the results shown in Table 2, our proposed method belongs to embedding-based methods, and
 364 achieves competitive results compared with the more complicated generative methods. Among the
 365 embedding-based methods, CF-ZIR achieves the best accuracy on AwA2 dataset, and second accu-
 366 racy on aPY and AwA1 datasets.

367 4.3 ABLATION STUDIES

369 In order to demonstrate the effectiveness of each component in CF-ZIR, including the discrimination
 370 loss and the learning of image-semantic coupled dictionary, we design several ablation experiments
 371 on the three datasets. The results of ablation experiments are shown in Table 3.

372 **Discrimination Loss:** By comparing the CF-ZIR w/o DL and CF-ZIR in Table 3 row 1 and row 3,
 373 adding the discrimination loss brings improvements on the three datasets, especially on the AwA2
 374 dataset. This phenomenon indicates that using discriminative loss can constrain the discriminability
 375 of cross domain dictionary pairs, thereby facilitating the recognition of unseen class images.

377 **Visual-Semantic Alignment:** The row 2 and row 3 in Table 3 show the results of ablation experi-
 378 ments on whether visual-semantic alignment, the CF-ZIR w/o VSA and CF-ZIR. Note that instead

378
 379 Table 2: Recognition accuracies (unit: %) of CF-ZIR vs comparative methods on aPY, AwA1 and
 380 AwA2 datasets. The best and second-best results are marked in **Red** and **Blue**, respectively. “*”
 381 indicates the methods of adopting attribute features.

Type	Methods	aPY	AwA1	AwA2
Generative	CCSS Liu et al. (2018a)	35.5	56.3	63.7
	RAS-cGAN Zhang et al. (2019)	40.1	67.4	-
	LisGAN Li et al. (2019)	43.1	70.6	-
	EDE Zhang et al. (2020)	20.4	70.1	66.5
	ACGN Liu et al. (2021)	44.4	69.2	69.7
	CE-GZSL Han et al. (2021)	-	71.0	70.4
Embedding-based	GAZSL Zhang et al. (2018)	41.2	68.3	70.2
	DCN Liu et al. (2018b)	43.6	65.2	-
	CDL Jiang et al. (2018)	43.0	69.9	68.2
	HSVA Chen et al. (2021b)	-	70.6	-
	TransZero* Chen et al. (2022a)	-	-	70.1
	MSDN* Chen et al. (2022b)	-	-	70.1
	ERPCNet Li et al. (2022)	43.5	-	71.8
	HCDDL Li et al. (2023)	50.6	71.8	70.8
	IAAC-net Chen & Zhou (2024)	-	-	70.7
	RSR Liu et al. (2024)	45.4	-	68.4
CF-ZIR		48.0	71.5	72.0

401
 402
 403 Table 3: Results of ablation experiments, Discrimination Loss (DL), Visual-Semantic Align-
 404 ment(VSA).

Model	aPY	AwA1	AwA2
CF-ZIR w/o DL	47.7	70.9	70.4
CF-ZIR w/o VSA	46.0	67.5	66.0
CF-ZIR	48.0	71.5	72.0

413 of using visual-semantic alignment, the semantic vectors of the unseen class images are generated
 414 based on the common visual feature dictionary learned in the first stage, and the class semantic vec-
 415 tors closest to these vectors are found to predict the categories of the unseen class images. We can
 416 see that using visual-semantic alignment outperforms without it on the three datasets, especially by
 417 4.0% and 6.0% on AwA1 and AwA2 datasets, respectively.

420 4.4 FURTHER ANALYSIS

422 This subsection analyzes the quality of image semantic vectors generated by CF-ZIR. High quality
 423 image semantic vectors help to learn better visual semantic cross domain dictionary pairs, ensuring
 424 the accuracy of visual semantic mapping. Therefore, in order to analyze the quality of image seman-
 425 tic vectors generated by CF-ZIR more intuitively, we visualizes the seen visual features of images
 426 and their corresponding image semantic vectors separately. Using the unsupervised dimensionality
 427 reduction method t-SNE, project high-dimensional vectors into a two-dimensional space.

428 As shown in Fig. 2, compared with the visual feature distribution of the image in the top line, the
 429 semantic vector distribution of the image in the bottom line exhibits more obvious intra class clus-
 430 tering and inter class dispersion. This not only indicates that the image semantic vectors generated
 431 by CF-ZIR are reasonable and reliable, but also shows that the image semantic vectors are of high
 quality, which is conducive to the establishing of visual semantic alignment.

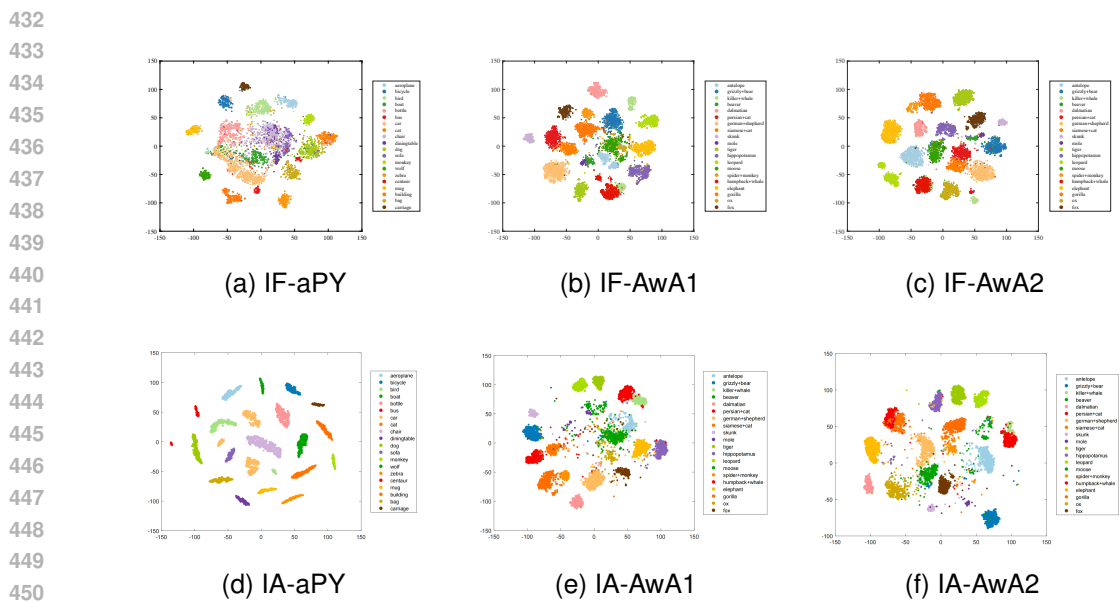


Figure 2: T-SNE visualization of the seen image features and the generated image attributes from aPY, AwA1 and AwA2 datasets (randomly selected several classes).

5 CONCLUSION

This paper proposed a common feature learning method for zero-shot image recognition (CF-ZIR), innovatively segmented into visual attribute and visual semantic embedding stages. By extracting common visual features and achieving cross-domain alignment between visual and semantic spaces, CF-ZIR adeptly captures the subtleties essential for recognizing classes not encountered during training. The method’s efficacy is underscored by its exceptional performance on three major benchmark datasets, with ablation studies confirming the pivotal role of the discriminative term loss and cross-domain alignment in bolstering recognition accuracy.

REFERENCES

- Shiming Chen, Wenjie Wang, Beihao Xia, Qinmu Peng, Xinge You, Feng Zheng, and Ling Shao. FREE: feature refinement for generalized zero-shot learning. In *Proceedings of the IEEE International Conference on Computer Vision*, pp. 122–131. IEEE, 2021a.
- Shiming Chen, Guo-Sen Xie, Qinmu Peng, Yang Liu, Baigui Sun, Hao Li, Xinge You, and Ling Shao. HSVA: hierarchical semantic-visual adaptation for zero-shot learning. In *Advances in Neural Information Processing Systems*, pp. 16622–16634, 2021b.
- Shiming Chen, Ziming Hong, Yang Liu, Guo-Sen Xie, Baigui Sun, Hao Li, Qinmu Peng, Ke Lu, and Xinge You. Transzero: Attribute-guided transformer for zero-shot learning. In *Conference on Artificial Intelligence*, pp. 330–338, 2022a.
- Shiming Chen, Ziming Hong, Guo-Sen Xie, Wenhao Wang, Qinmu Peng, Kai Wang, Jian Zhao, and Xinge You. MSDN: mutually semantic distillation network for zero-shot learning. In *Proceedings of the IEEE Conference on Computer Vision and Pattern Recognition*, pp. 1–10, 2022b.
- Yuan Chen and Yuan Zhou. Incorporating attribute-level aligned comparative network for generalized zero-shot learning. *Neurocomputing*, 573(127188):1–1, 2024.
- A. Farhadi, I. Endres, D. Hoiem, and D. Forsyth. Describing objects by their attributes. In *Proceedings of the IEEE Conference on Computer Vision and Pattern Recognition*, pp. 1778–1785, 2009.

- 486 Ian J. Goodfellow, Jean Pouget-Abadie, Mehdi Mirza, Bing Xu, David Warde-Farley, Sherjil Ozair,
 487 Aaron C. Courville, and Yoshua Bengio. Generative adversarial nets. In *Advances in Neural*
 488 *Information Processing Systems*, pp. 2672–2680, 2014.
- 489
- 490 Zongyan Han, Zhenyong Fu, Shuo Chen, and Jian Yang. Contrastive embedding for generalized
 491 zero-shot learning. In *Proceedings of the IEEE Conference on Computer Vision and Pattern*
 492 *Recognition*, pp. 2371–2381, 2021.
- 493 Kaiming He, Xiangyu Zhang, Shaoqing Ren, and Jian Sun. Deep residual learning for image recog-
 494 nition. In *Proceedings of the IEEE Conference on Computer Vision and Pattern Recognition*, pp.
 495 770–778, 2016.
- 496
- 497 Zhong Ji, Junyue Wang, Yunlong Yu, Yanwei Pang, and Jungong Han. Class-specific synthesized
 498 dictionary model for zero-shot learning. *Neurocomputing*, 329:339–347, 2019.
- 499
- 500 Huajie Jiang, Ruiping Wang, Shiguang Shan, and Xilin Chen. Learning class prototypes via structure
 501 alignment for zero-shot recognition. In *European Conference on Computer Vision*, volume 11214,
 502 pp. 121–138, 2018.
- 503
- 504 Christoph H. Lampert, Hannes Nickisch, and Stefan Harmeling. Learning to detect unseen object
 505 classes by between-class attribute transfer. In *IEEE Computer Society Conference on Computer*
Vision and Pattern Recognition, pp. 951–958, 2009.
- 506
- 507 Hugo Larochelle, Dumitru Erhan, and Yoshua Bengio. Zero-data learning of new tasks. In *Confer-
 ence on Artificial Intelligence*, pp. 646–651, 2008.
- 508
- 509 Jingjing Li, Mengmeng Jing, Ke Lu, Zhengming Ding, Lei Zhu, and Zi Huang. Leveraging the in-
 510 variant side of generative zero-shot learning. In *Proceedings of the IEEE Conference on Computer*
Vision and Pattern Recognition, pp. 7402–7411, 2019.
- 511
- 512 Shuang Li, Lichun Wang, Shaofan Wang, Dehui Kong, and Baocai Yin. Hierarchical coupled dis-
 513 criminative dictionary learning for zero-shot learning. *IEEE Transactions on Circuits and Systems*
 514 *for Video Technology*, pp. 1–1, 2023. doi: 10.1109/TCSVT.2023.3246475.
- 515
- 516 Yun Li, Zhe Liu, Lina Yao, Xianzhi Wang, Julian J. McAuley, and Xiaojun Chang. An entropy-
 517 guided reinforced partial convolutional network for zero-shot learning. *IEEE Transactions on*
Circuits and Systems for Video Technology, 32(8):5175–5186, 2022.
- 518
- 519 Jinlu Liu, Xirong Li, and Gang Yang. Cross-class sample synthesis for zero-shot learning. In *British*
 520 *Machine Vision Conference*, pp. 1–12, 2018a.
- 521
- 522 Jinlu Liu, Zhaocheng Zhang, and Gang Yang. Cross-class generative network for zero-shot learning.
 523 *Information Sciences*, 555:147–163, 2021.
- 524
- 525 Shichen Liu, Mingsheng Long, Jianmin Wang, and Michael I. Jordan. Generalized zero-shot learn-
 526 ing with deep calibration network. In *Advances in Neural Information Processing Systems*, pp.
 527 2009–2019, 2018b.
- 528
- 529 Zhe Liu, Yun Li, Lina Yao, Julian J. McAuley, and Sam Dixon. Rethink, revisit, revise: A spiral
 530 reinforced self-revised network for zero-shot learning. *IEEE Trans. Neural Networks Learn. Syst.*,
 35(1):657–669, 2024.
- 531
- 532 Mehdi Mirza and Simon Osindero. Conditional generative adversarial nets. *Computer Science*, pp.
 2672–2680, 2014.
- 533
- 534 Alec Radford, Jong Wook Kim, Chris Hallacy, Aditya Ramesh, Gabriel Goh, Sandhini Agar-
 535 wal, Girish Sastry, Amanda Askell, Pamela Mishkin, Jack Clark, Gretchen Krueger, and Ilya
 536 Sutskever. Learning transferable visual models from natural language supervision. In *Proceed-
 537 ings of the 38th International Conference on Machine Learning*, volume 139, pp. 8748–8763,
 2021.
- 538
- 539 Jiayi Shen, Zehao Xiao, Xiantong Zhen, and Lei Zhang. Spherical zero-shot learning. *IEEE Trans-
 actions on Circuits and Systems for Video Technology*, 32(2):634–645, 2022.

- 540 Ziyang Wang, Yunhao Gou, Jingjing Li, Lei Zhu, and Heng Tao Shen. Language-augmented pixel
 541 embedding for generalized zero-shot learning. *IEEE Transactions on Circuits and Systems for*
 542 *Video Technology*, pp. 1–1, 2022. doi: 10.1109/TCSVT.2022.3208256.
- 543 Jiamin Wu, Tianzhu Zhang, Zheng-Jun Zha, Jiebo Luo, Yongdong Zhang, and Feng Wu. Self-
 544 supervised domain-aware generative network for generalized zero-shot learning. In *IEEE Con-*
 545 *ference on Computer Vision and Pattern Recognition*, pp. 12764–12773, 2020.
- 546 Yongqin Xian, Bernt Schiele, and Zeynep Akata. Zero-shot learning - the good, the bad and the
 547 ugly. In *Proceedings of the IEEE Conference on Computer Vision and Pattern Recognition*, pp.
 548 3077–3086, 2017.
- 549 Yongqin Xian, Tobias Lorenz, Bernt Schiele, and Zeynep Akata. Feature generating networks for
 550 zero-shot learning. In *Proceedings of the IEEE Conference on Computer Vision and Pattern*
 551 *Recognition*, pp. 5542–5551, 2018.
- 552 Yongqin Xian, Christoph H. Lampert, Bernt Schiele, and Zeynep Akata. Zero-shot learning - A com-
 553 prehensive evaluation of the good, the bad and the ugly. *IEEE Transactions on Pattern Analysis*
 554 and *Machine Intelligence*, 41(9):2251–2265, 2019.
- 555 Hairui Yang, Baoli Sun, Baopu Li, Caifei Yang, Zhihui Wang, Jenhui Chen, Lei Wang, and Haojie
 556 Li. Iterative class prototype calibration for transductive zero-shot learning. *IEEE Transactions on*
 557 *Circuits and Systems for Video Technology*, pp. 1–1, 2022. doi: 10.1109/TCSVT.2022.3209209.
- 558 Haofeng Zhang, Yang Long, and Ling Shao. Zero-shot hashing with orthogonal projection for image
 559 retrieval. *Pattern Recognition Letters*, 117:201–209, 2018.
- 560 Haofeng Zhang, Yang Long, Li Liu, and Ling Shao. Adversarial unseen visual feature synthesis for
 561 zero-shot learning. *Neurocomputing*, 329:12–20, 2019.
- 562 Lei Zhang, Peng Wang, Lingqiao Liu, Chunhua Shen, Wei Wei, Yanning Zhang, and Anton van den
 563 Hengel. Towards effective deep embedding for zero-shot learning. *IEEE Transactions on Circuits*
 564 and *Systems for Video Technology*, 30(9):2843–2852, 2020.
- 565 Xiaojie Zhao, Yuming Shen, Shidong Wang, and Haofeng Zhang. Boosting generative zero-shot
 566 learning by synthesizing diverse features with attribute augmentation. In *Conference on Artificial*
 567 *Intelligence*, pp. 3454–3462, 2022.
- 568
 569
 570
 571
 572
 573
 574
 575
 576
 577
 578
 579
 580
 581
 582
 583
 584
 585
 586
 587
 588
 589
 590
 591
 592
 593